SLIDING MODE VECTOR CONTROL OF A PWM INVERTER FED INDUCTION MOTOR

Aymen A. Salih
Mechatronics Engineering Dept.
University of Baghdad

Prof. Dr. Qais S. Al-Sabbagh
Computer Engineering Dept.
University of Baghdad

Asst. Prof. Azzam M. Ahmed
Information Engineering Dept.
University of Baghdad

ABSTRACT

The purpose of this paper is to analyze, study and simulate a three-phase induction motor drive using vector (field-oriented) control strategy and PWM current regulated inverter using hysteresis band current controller. The mathematical model of the induction motor and the principle of indirect field-oriented control are introduced. The Sliding Mode Controller with Boundary Layer (SMC-BL) is used as a speed controller and compared with the proportional integral (PI) controller.
A Simulink / Matlab program is written for simulating the induction motor model, SMC-BL and PI controllers and indirect field oriented control. The SMC-BL based system and PI-controller based system are compared from the point of view of speed–time response and load disturbance.
The simulation results which illustrate the performance of SMC-BL based system and PI-controller based system are plotted and discussed. These results obtained have shown improvement in the SMC-BL system performance from the point of view of variable speed tracking and load disturbance.

KEY WORD
induction motor, field oriented control, sliding mode control.

الخلاصة

الهدف من هذا البحث هو تحليل ودراسة ومحاكاة مسوق تيارمتناوب لمحرك حثي ثلاثي الطور باستخدام ستراتيجية السيطرة على اتجاه المجال(FOC) وباستخدام عاكس التيارالعامل بتضمين عرض الموجة (PWM current regulated inverter) المستخدم لمسيطر التيار المتضمن حزمة الهسترة (Hysteresis band current controller).تم تقديم النموذج الرياضي للمحرك الحثي ومباديء سيطرة المجال(FO) غير المباشر. تم أستخدام المسيطر الانزلاقي ذو المحددات (SMC-BL) كمسيطر للسرعة ومقارنتة مع المسيطر التناسبي التكاملي (PI).
استخدم برنامج (Simulink / Matlab) لمحاكاة وتمثيل نموذج المحرك الحثي و المسيطرات (SMC-BL) و (PI) و المسيطر الاتجاهي الغير مباشر(IFOC). وتمت المقارنة بين النتائج المستحصلة من تطبيق المسيطرات (SMC-BL) و (PI) من حيث الاستجابة الزمنية للسرعة وتأثيرأظطرابات الحمل (load disturbance) على السرعة.

تم رسم ومناقشة النتائج المستحصلة من المحاكاة والمتضمنة خصائص المنظومة الجديدة والمنظومة القديمة. أن النتائج النظرية اوضحت ان المنظومة الحديثة والتي تستخدم المسيطر الانزلاقي ذو المحددات هي جيدة جدا وهي افضل من المنظومة القديمة من ناحية الاستجابة الزمنية للسرع المختلفة وكذلك كبح تأثير الحمل على السرعة.

INTRODUCTION

The main types of motors that are used in speed control are dc motors and induction motors (IMs). The induction motors particularly the cage type are the most commonly used in industry due to their advantages over the dc motors. The main advantage is that induction motors do not require an electrical connection between stationary and rotating parts of the motor. Therefore, they do not need any mechanical commutator and brushes leading to the fact that they are maintenance free motors. Induction motors are cheap, robust, rugged structure, high efficiency (up to 80% higher) furthermore the induction motors can work in explosive environments because no sparks are produced.

However, the use of induction motors has several disadvantages; these include difficult controllability due to the complex mathematical model of the motors. Their nonlinear behavior during saturation, and variations of the electrical parameters due to the physical influence of temperature and a strong temperature dependency of electrical motor parameters. . For example, the rotor time constant of an induction motor can change up to 70% over a motor's temperature range. These factors make mathematical modeling of motor control systems difficult [1].

However, because of its highly non-linear and coupled dynamic structure, an induction motor requires more complex control schemes, more expensive and higher rated power converters than DC and permanent magnet motors [2].

Traditional open-loop control of the induction motors with variable frequency may provide a satisfactory solution under limited conditions. However, when high performance dynamic operation is required, these methods are unsatisfactory. Therefore, more sophisticated control methods are needed to make the performance of the induction motor comparable with DC motors such as Vector Control method.

MATHEMATICAL MODEL OF INDUCTION MOTOR

In an adjustable-speed drive the machine normally constitutes an element within a feedback loop, and therefore its transient behavior has to be taken into consideration. Besides high-performance drive control, such as vector- or field-oriented control, is based on the dynamic d-q model of the machine.

The dynamic performance of an AC machine is somewhat complex because of the three-phase rotor windings move with respect to three-phase stator windings, as shown in Figure (1 a). It can be looked on as transformer with a moving secondary coil, where the coupling coefficients between the stator and rotor phases change continuously with the change of the rotor position θ_r. The machine model can be described by differential equations with time-varying mutual inductances, but such a model tends to be very complex. A three-phase machine can be represented by an equivalent two-phase machine by using axes transformation Clark's transformation as shown in Figure (1 b), where $d^s - q^s$ correspond to stator direct and quadrature axes, $d^r - q^r$ to rotor direct and quadrature axes. This will reduce the order of the differential equations describing the machine. However, the problem of time-varying parameters still remains. This problem can be solved by replacing the machine variables (voltages, currents, and flux linkage) associated with stator windings that are fixed to stationary axes (frame) with variables associated with fictitious windings fixed to axes rotate at synchronous speed. This is called Park's transformation from stationary reference frame to synchronously rotating reference frame. This transformation will eliminates all

the time varying inductances due to the relative motion between stator and rotor electric circuit and varying magnetic reluctances [1].

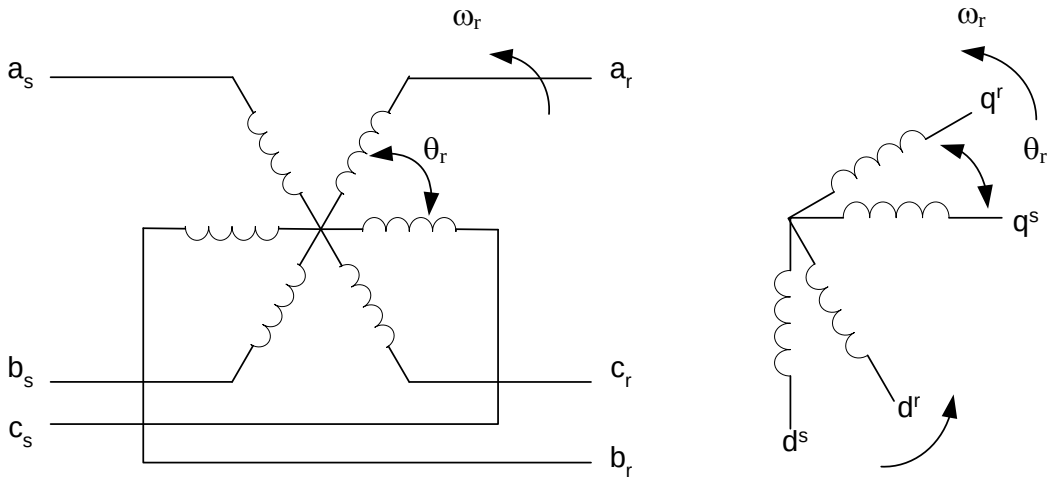

Fig (1) (a) Coupling effect in three-phase stator and rotor windings of motor, (b) Equivalent two-phase machine [1].

The mathematical model of a three phase induction motor and load is described by equations in the synchronously rotating reference frame (d^e - q^e) as [1]:

$$\begin{bmatrix} v_{qs} \\ v_{ds} \\ v_{qr} \\ v_{dr} \end{bmatrix} = \begin{bmatrix} R_s + sL_s & \omega_e L_s & sL_m & \omega_e L_m \\ -\omega_e L_s & R_s + sL_s & -\omega_e L_m & sL_m \\ sL_m & (\omega_e - \omega_r)L_m & R_r + sL_r & (\omega_e - \omega_r)L_r \\ -(\omega_e - \omega_r)L_m & sL_m & -(\omega_e - \omega_r)L_r & R_r + sL_r \end{bmatrix} \begin{bmatrix} i_{qs} \\ i_{ds} \\ i_{qr} \\ i_{dr} \end{bmatrix} \quad \textbf{(1)}$$

Where s is a d/dt operator.

For singly-fed machine (i.e. only stator be energized) such as squirrel cage motor, $v_{qr} = v_{dr} = 0$. The speed ω_r in Equation (1) can be related to the torque as:

$$T_e = T_L + J\frac{d\omega_m}{dt} = T_L + \frac{2}{P}J\frac{d\omega_r}{dt} \quad \textbf{(2)}$$

Where

$$T_e = \frac{3}{2}\left(\frac{P}{2}\right)L_m\left(i^e_{qs}i^e_{dr} - i^e_{ds}i^e_{qr}\right) \quad \textbf{(3)}$$

And

T_e = Developed or electromagnetic torque, T_L = load torque, P = Number of poles of the motor J = rotor inertia, ω_r = rotor speed in electrical rad/sec and ω_m = rotor mechanical speed.

Equations (1)-(3) give the complete model of the electro-mechanical dynamics for induction machine in synchronous frame.

VECTOR CONTROL

Field oriented control transforms the dynamic structure of the ac machine into that of separately excited DC machine. For a DC machine, the field flux is proportional to the field current assuming that the magnetic saturation term is negligible. If the field is assumed to be constant and independent of armature current, the armature current provides direct control of torque, so that [3]:

$$T_e \propto I_f \times I_a \quad \textbf{(4)}$$

With the induction motor transformed to *d-q* plane, it looks like a separately exited DC machine and it can achieve four quadrant operations with fast torque response and satisfactory performance down to standstill. The space angle of the induction motor (angle between stator and rotor fields) will vary with load and; therefore, result in complex interactions between the fields. The space angle will be controlled such that the stator input current can be decoupled into flux producing (i_{ds}^s) and torque producing (i_{qs}^s) components.

There are two essentially general methods of vector control. One is called the direct or feedback method, and the other is known as the indirect or feedforward method [1]. These methods are different essentially by how the unit vector ($\cos\theta_e$ and $\sin\theta_e$) is generated for the control. It should be mentioned that the orientation of i_{ds}^e with the rotor flux λ_r, air gap flux λ_m, or stator flux λ_s is possible in vector control. However, rotor flux orientation gives natural decoupling control, whereas air gap or stator flux orientation gives a coupling effect which has to be compensated by a decoupling compensation current.

Indirect vector control method is essentially the same as direct vector control, except the unit vector signals ($\cos\theta_e$ and $\sin\theta_e$) are generated in feedforward manner. Indirect vector control is very popular in industrial applications. The fundamental principle of indirect vector control can be explained by a phasor diagram shown in Figure (2). The $d^s - q^s$ axes are fixed on the stator, but the $d^r - q^r$ axes, which are fixed on the rotor, are moving at speed ω_r as shown. Synchronously rotating axes $d^e - q^e$ are rotating ahead of the $d^r - q^r$ axes by the positive slip angle θ_{sl} corresponding to slip frequency ω_{sl}.

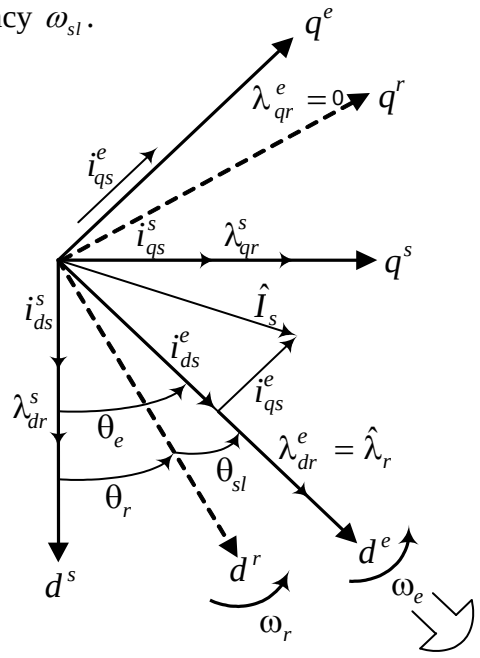

Fig (2) Phasor diagram explaining indirect vector control [1]

Since the rotor pole is directed on the d^e axis and $\omega_e = \omega_r + \omega_{sl}$, one can write

$$\theta_e = \int \omega_e dt = \int (\omega_r + \omega_{sl}) dt = \theta_r + \theta_{sl} \quad \textbf{(5)}$$

The phasor diagram suggests that for decoupling control, the stator flux component of current i_{ds}^e should be aligned on the d^e axis, and the torque component of current i_{qs}^e should be on the q^e axis.

To implement the indirect vector control strategy, equation (5) and the following equations should be applied [1]:

$$\frac{L_r}{R_r}\frac{d\hat{\lambda}_r}{dt} + \hat{\lambda}_r = L_m i_{ds}^e \quad \textbf{(6)}$$

$$\omega_{sl} = \frac{L_m R_r}{L_r \hat{\lambda}_r} i_{qs}^e \quad \textbf{(7)}$$

$$T_e = \frac{3}{2}\frac{P}{2}\frac{L_m}{L_r}\lambda_{dr}^e i_{qs}^e \quad \textbf{(8)}$$

The unit vector signals $\cos\theta_e$ and $\sin\theta_e$ are obtained from the angle θ_e by integrating ω_e signal.

VARIABL STRUCTURE WITH SLIDING MODE CONTROL

Variable structure systems (VSS) with a sliding mode (SMC) were discussed first in the Soviet literature [4,5], and have been widely developed in recent years. Comprehensive survey of variable structure control can be found in [6, 7].

VSS with SMC are characterized by control laws that are discontinuous on a certain manifold in the state space, the so-called sliding surface [5,8]. A VSS control law is designed such that the representative point's trajectories of the closed-loop system are attracted to the sliding surface and once on the sliding surface they slide towards the origin Fig (3) [9]. The dynamic performance of SMC has been confirmed to be an effective robust control approach as facing the problems of systems uncertainties and unknown disturbances, but a SMC indeed exhibits some drawbacks [10]. The major drawback in the SMC approach is the undesired phenomenon of chattering Fig (3), because of the discontinuous change of control laws across the sliding surface. In practical engineering systems, chattering may cause damage to system components, as well as excite unmodelled and high frequency plant dynamics [11].

There exist several techniques to eliminate chattering. The widely-adopted approach to chattering-free VSS is the so-called boundary layer, where the discontinuous VSS control law signum function is applied to small vicinity around the sliding surface (see [7,12]).

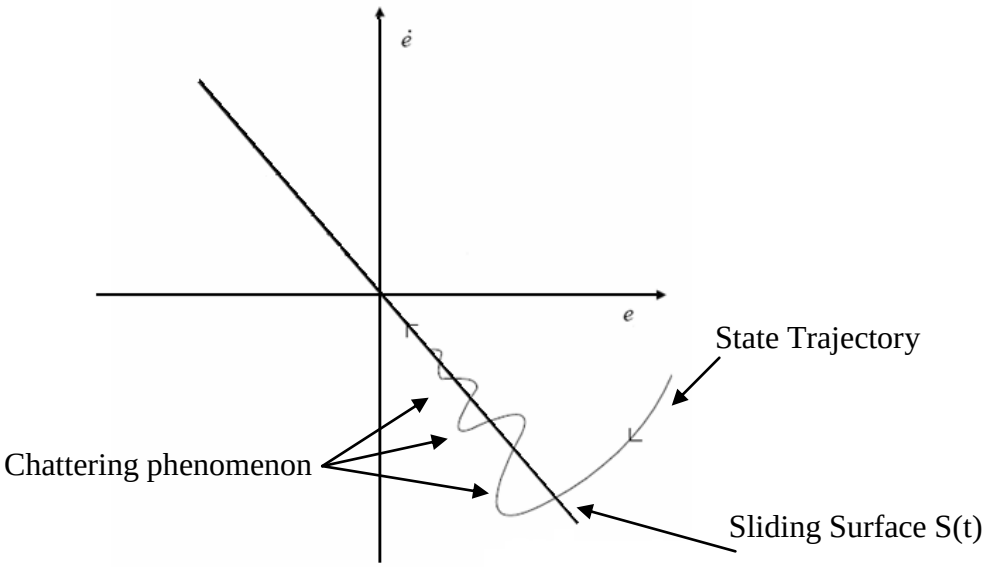

Fig (3) Sliding motion of the system

SLIDIN MODE CONTROLLER DESIGN

The sliding mode control consists of two phases [13]:

- Designing an equilibrium surface, called sliding surface S(t), such that any state trajectory of the plant restricted to the sliding surface is characterized by the desired behavior.
- Designing a discontinuous control law to force the system to move on the sliding surface in a finite time

.

Sliding mode control Law

To apply the SMC approach, we first define a time-varying sliding surface, S(t), in the state space R^n by the vector equation $S(e,e^{\bullet})=0$, where

$$S(t)=Ce+e^{\bullet} \qquad \textbf{(9)}$$

Where *C* is a strictly positive constant number, and e , $\dot{e}$ is the state tracking errors and their time derivatives respectively.

Sliding mode means that once the state trajectory has reached the sliding surface *S*=0 the system trajectory remains on it while sliding into the origin (*e*=0) independently of model uncertainties, unmodeled frequencies, and disturbances [13]. So, the SMC is known as being robust for model parameter variations. This property is used for compensating the effects of model uncertainties and load disturbances [14]. For the induction motor speed control, let $e=\omega_{ref}-\omega$ and $e^{\bullet}=\omega^{\bullet}{}_{ref}-\omega^{\bullet}$, where ($\omega_{ref}$) is the motor reference speed, and (ω) is the motor actual speed.

As can be seen from Eq. (9), maintaining system states on the surface $S(e,\dot{e})=0$ for all (*t* > 0) will "closely" satisfy the tracking requirements $\omega\rightarrow\omega_{ref}$ and $\omega^{\bullet}\rightarrow\omega^{\bullet}{}_{ref}$. Indeed, it will force e and $\dot{e}$ to approach zero, given any bounded initial conditions *e*(0) and $\dot{e}(0)$.

By choosing the Lyapunov function candidate $V=0.5S^{T}S$, a reaching condition (sliding condition) is obtained as [15]:

$$\dot{V} = S^T \dot{S}; S \neq 0 \quad \text{or} \qquad \textbf{(10 a)}$$

$$S^T \dot{S} \leq -\alpha \left| S^T \right| = -\alpha S^T \operatorname{sgn}(S) \qquad \textbf{(10 b)}$$

Where α is a strictly positive constant. Reaching the sliding mode means a system trajectory is outside the sliding surface but follows the reaching condition Eq.(10 b) [15].

Essentially, Eq.(10 b) states that the squared "distance" to the surface, as measured by $S^T \dot{S}$, decreases along all system trajectories. Thus, Eq. (10 b) provides a sufficient reaching condition such that the tracking error e will asymptotically converge to zero [14].
The sliding mode controller law is now chosen as follows:

$$u_{smc} = K \operatorname{sgn}(S) \qquad \textbf{(11)}$$

Where

$$S(t) = Ce + \dot{e}$$

K: +ve constant number,

$$\operatorname{sgn}(S) = \begin{cases} -1 & \text{if } S < 0 \\ +1 & \text{if } S > 0 \end{cases} \qquad \textbf{(12)}$$

The state trajectories with signum function is shown in Fig (4).

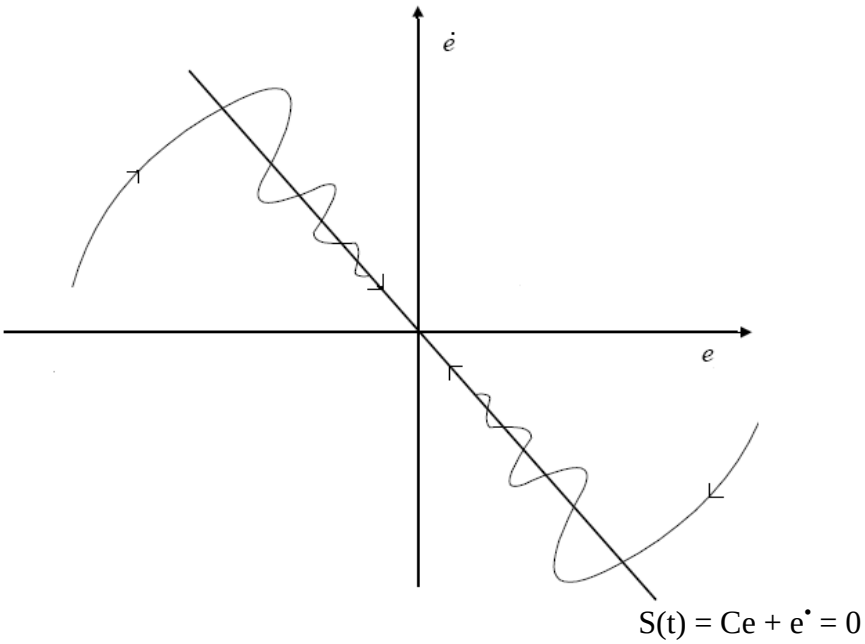

Fig (4) State trajectories with signum function [6]

Saturation Function Instead of Signum Function

To eliminate the chattering phenomenon caused by the signum function, Saturation function is used. This method is called SMC with boundary layer (BL). For each link, define thin boundary layers (BL) neighboring the sliding surfaces [12].

$$B_i(t) = \{q_i, \left| S_i(q,t) \right| \leq \Phi_i\}, \Phi_i > 0 \qquad i = 1, 2, 3\ldots \qquad \textbf{(13)}$$

Where $|S_i(q,t)|$ is the distance between state e_i and sliding surface S_i, Φ_i is the boundary layer thickness and, as illustrated in Fig. (5) for i=1 in the error phase space. To remedy the control discontinuity in the boundary layer, the signum function $(\mathrm{sgn}(s))$ is replaced by a saturation function of the form [16,10].

$$sat(S_i) = \begin{cases} \mathrm{sgn}(S_i), & if\ |S_i| \geq \Phi_i \\ \dfrac{S_i}{\Phi_i}, & if\ |S_i| < \Phi_i \end{cases} \qquad i = 1, 2, 3\ldots \qquad \textbf{(14)}$$

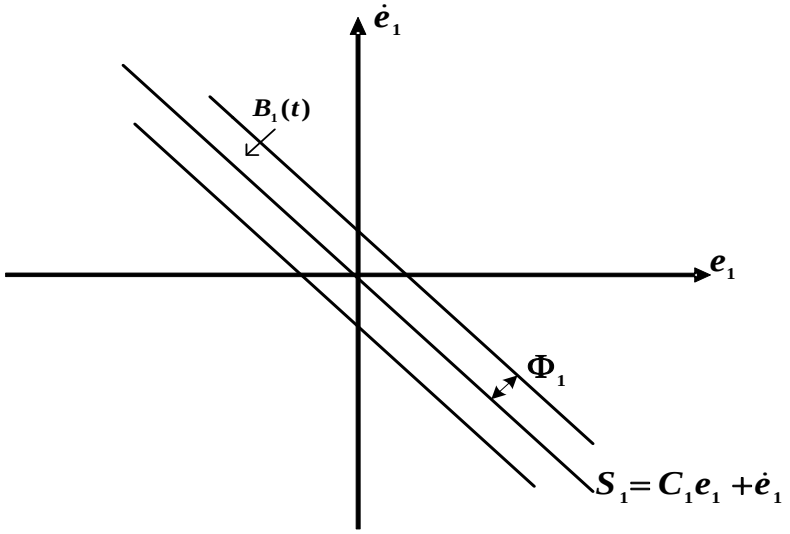

Fig (5) The sliding surface and the boundary layer [9].

However, the system state with this control law is uniform ultimate bounded with respect to a small neighborhood of the origin Fig (6) [17]. Let $\varepsilon_i = C_i^{-1}\Phi_i$, $i = 1,2,3,....$ be the boundary layer width. As shown in [18], the tracking errors exist within a guaranteed precision ε_i. Therefore, the larger the boundary layers the smaller the control chattering and the greater the tracking errors [10].

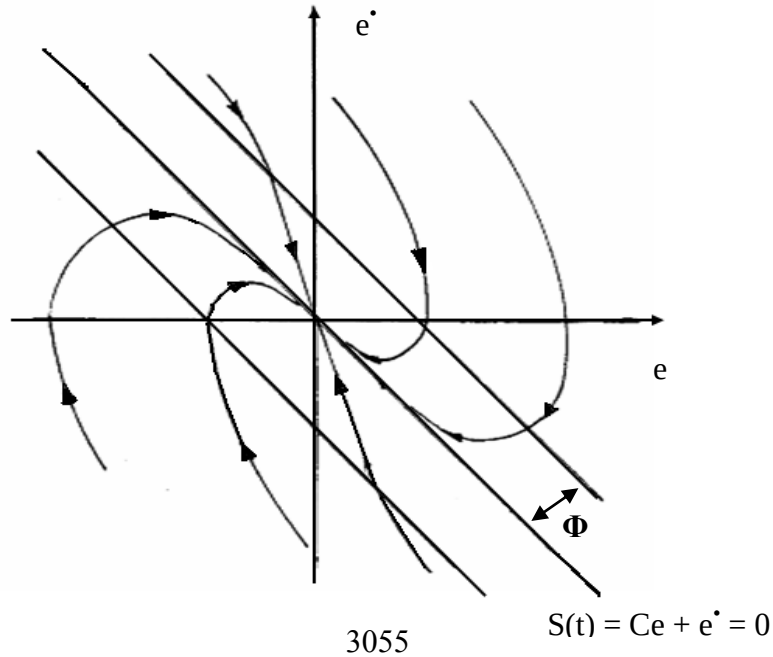

Fig (6) State trajectories with saturation function [17].

SIMULATIONS

Induction machines models are often ill – defined. Even if the machine model is well known, there may be a parameter variation problem. The *d-q* machine model discussed before was multivariable, complex, and nonlinear. Vector or Field Oriented Control of a drive can overcome this problem, but accurate vector control is nearly impossible. To overcome such problems Sliding Mode with boundary layer technique was used. The overall Simulink block diagram of the Vector Control of a three phase induction motor is shown in Fig. (7), which are taken from the MATLAB program.

The Field Oriented Control (FOC) makes the rotor shaft to follow or track the input reference speed (ω^*). The command speed signal subtracted from the measured rotor speed and generates the error signal. The error generated is then fed into a speed controller block. The speed controller block is either a Proportional Integral (PI) controller or a Sliding Mode Controller with Boundary Layer (SMC-BL) that generates a torque command (T_e^*). This torque command is used to set the electromagnetic torque induced within the induction motor by calculating an appropriate i_{qs}^* command based on the generated T_e^* signal according to Equation (8), and the flux will be computed from the resulting direct component of stator current (i_{ds}), and the flux is assumed to be constant when the motor is operated below and beyond the rated speed, and the flux-speed product is held constant. Inside the (FOC) block calculations are made and the reference direct and quadrature components of the stator current (i_{ds}^*, i_{qs}^*) are generated. These two components are fed to the (dq to abc) conversion block to generate the three phase reference currents (I_{abc}^*). These are then compared with the actual measured currents (I_{abc}) in the hysteresis band current regulator block to generate the pulses to feed the current source PWM inverter. The latter produces the driving power for a (50 Hp, 460 V, 60 Hz, 4 poles) three phase induction motor as shown in Fig. (8).

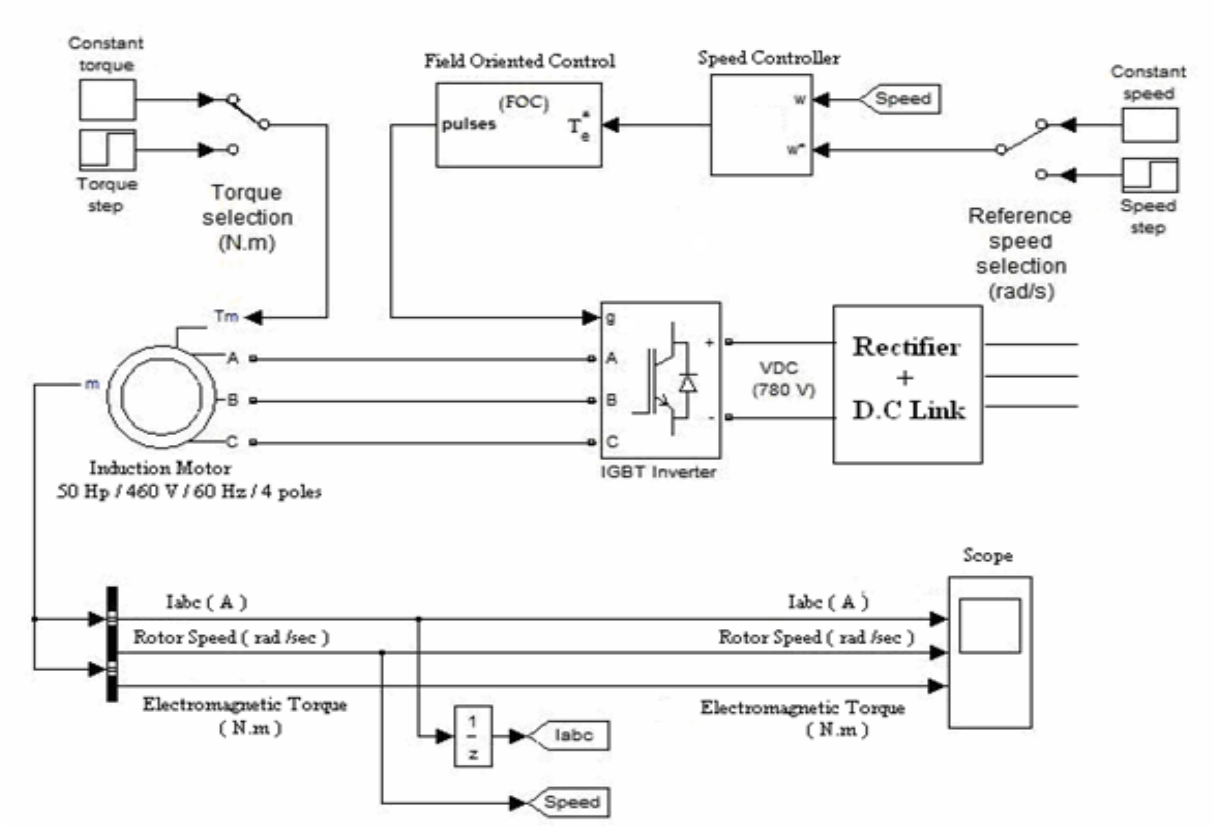

Fig (7) Overall control system [MATLAB].

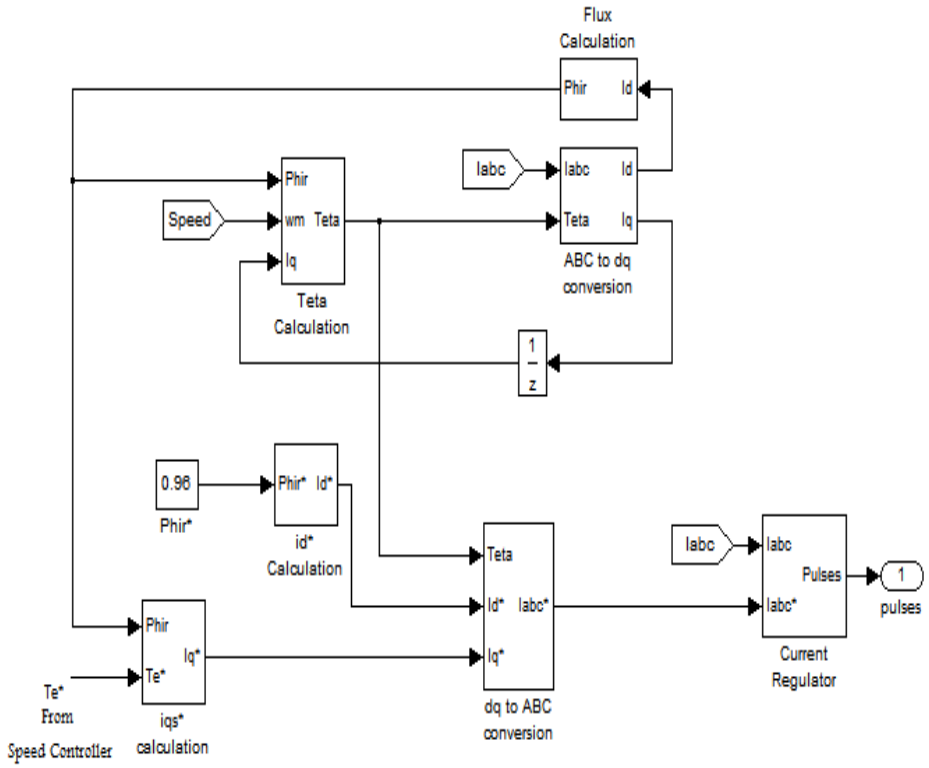

Fig (8) Inside field oriented control block [MATLAB].

SMC-BL Speed Controller Tuning

The control law of this controller is given as in equation (14):

U_{smc}= K sat (S)

Where

$$sat(S) = \begin{cases} \text{sgn}(S), & if\ |S| \geq \Phi \\ \dfrac{S}{\Phi}, & if\ |S| < \Phi \end{cases} \qquad \text{and} \qquad S(t) = Ce + \dot{e}$$

Controller parameters (K, C, and Φ) chosen should be made very carefully to satisfy the desired speed response without affecting the overall behavior of the system. Every parameter has specific effects on some region of the overall response. Where the gain (K) affects the initial starting point of the controlled variable, also it affects the transient response for the controlled system. The gain (C) affects the transient response and the steady state error, while the (Φ) parameter is used to eliminate the chattering phenomena.

For the controlled system (FOC-IM), if the value of (K) is small then the initial value of the electromagnetic torque (T_e) will be small. Then the transient response of the speed curve will be slow and it takes large time to reach steady state region, and vise versa as shown in Figures.(9, 10). If the value of (C) is small then the transient response of the speed curve will be slow and the steady state error will be large, and vise versa as shown in Figures.(11, 12). It should be noticed that there is a limit for increasing the values of (K, C) because it will no more affects the transient response but only increases the drawn currents and the electromagnetic torque at the instant of speed or torque changes during motor working.

The boundary layer (Φ) is used to eliminate the chattering, so it should be chosen small. If the boundary layer is very small then under some operating conditions chattering may re-occur. Alternatively, if the boundary layer is chosen large then chattering is completely eliminated. However, a large boundary layer results in slow system response and therefore degrades the dynamic performance of the system.

All the above tests are made on ω*=120 rad/sec, then the following values of the controller parameters are chosen to satisfy the desired speed response without affecting the overall behavior of the system:

K = 300, C = 18, Φ = 2

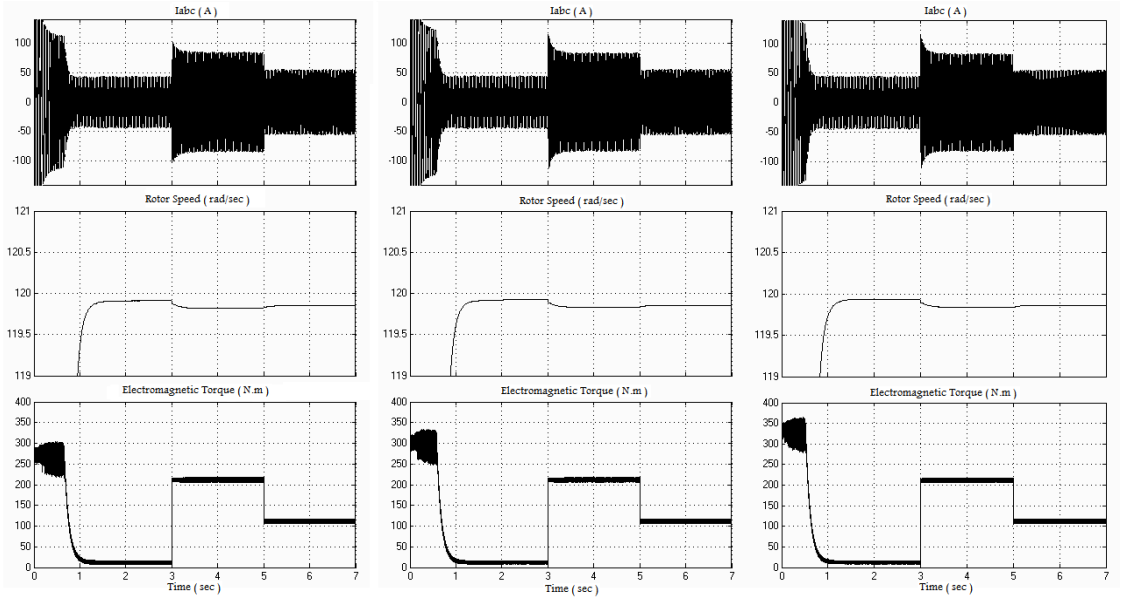

(a) K =270 (b) K= 300 (c) K= 330

Fig (9) Speed response at ω*=120 rad/sec with load step changes, at (t=3sec) from (0-200 N.m) and at (t=5sec) from (200-100 N.m).

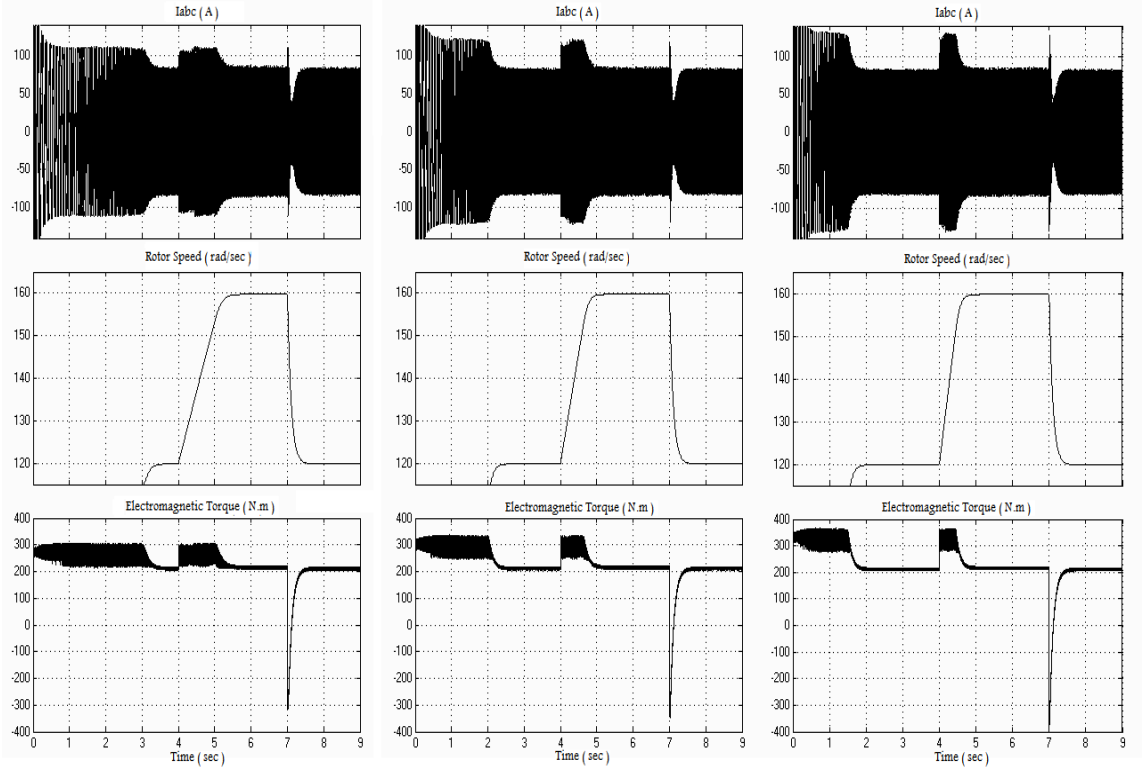

(a) K =270 (b) K= 300 (c) K= 330

Fig (10) Speed response at (200 N.m) load with speed step changes, at (t=4sec) from (120-160 rad/sec) and at (t=5sec) from (160-120 rad/sec).

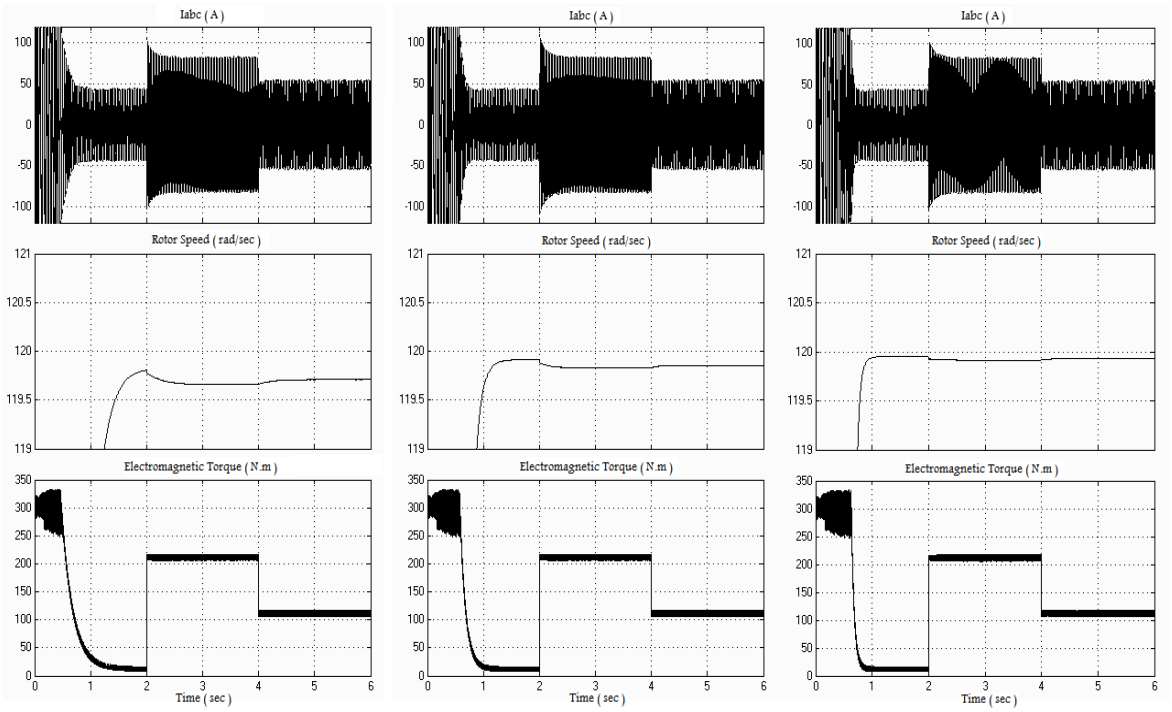

(a) C =5 (b) C= 10 (c) C= 20

Fig (11) Speed response at ω*=120 rad/sec with load step changes at (t=2sec) from (0-200 N.m) and at (t=4sec) from (200-100 N.m).

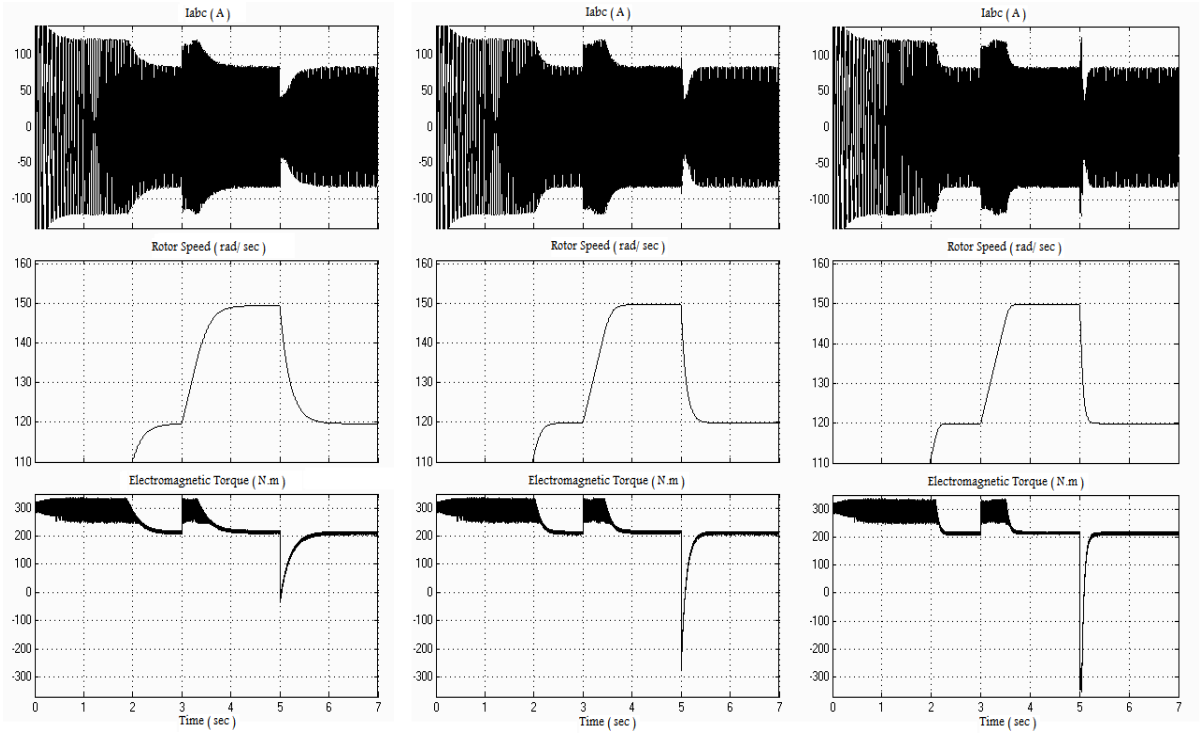

(a) C =5 (b) C= 10 (c) C= 20

Fig (12) Speed response at (200 N.m) load with speed step changes, at (t=3sec) from (120-150 rad/sec) and at (t=5sec) from (150-120 rad/sec).

RESULTS

In this section the results of simulation of sliding mode controller with boundary layer (SMC-BL) based on rotor field orientation induction motor drive are presented and discussed, also the results of simulation of conventional proportional integral (PI) controller for the same induction motor are presented and compared with the results of (SMC-BL) system from the point of view of speed tracking and load disturbance rejection on system response.
The simulation results will consist of two parts. The first part will show the System performance under no load. The second part will show the System performance under load. The parameters of the induction motor are listed in table (1):

Table (1) Parameters of induction motor.

Motor Power	50Hp
Frequency	60 Hz
Number of Poles	4
Volts	460 V
Stator resistance (R_s)	0.087 Ω
Rotor resistance (R_r)	0.228 Ω
Stator inductance (L_s)	0.8 mh
Rotor inductance (L_r)	0.8 mh
Magnetizing inductance (L_m)	34.7 mh
Friction constant (F)	0.1 N.m.s
Moment of inertia (J)	1.662 $Kg.m^2$

System Performance under No Load Conditions

Fig. (13) and Fig. (14) show the speed tracking performance under no load for two rated speeds (120 rad/sec), (30 rad/sec) respectively for both (SMC-BL) system and (PI) system. The motor speed (ω_r) tracks the reference model output (SMC-BL) system without overshoot, and the amount of torque ripple is much less than that of the (PI) system.

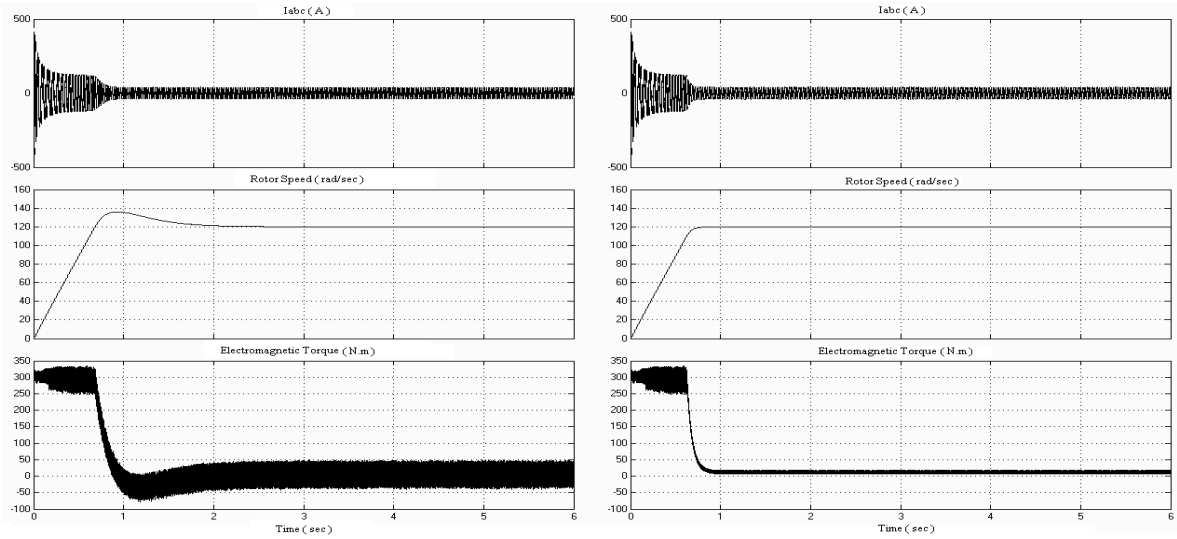

(a) PI (b) SMC-BL

Fig (13) Speed response at ω^*=120 rad/sec with no load

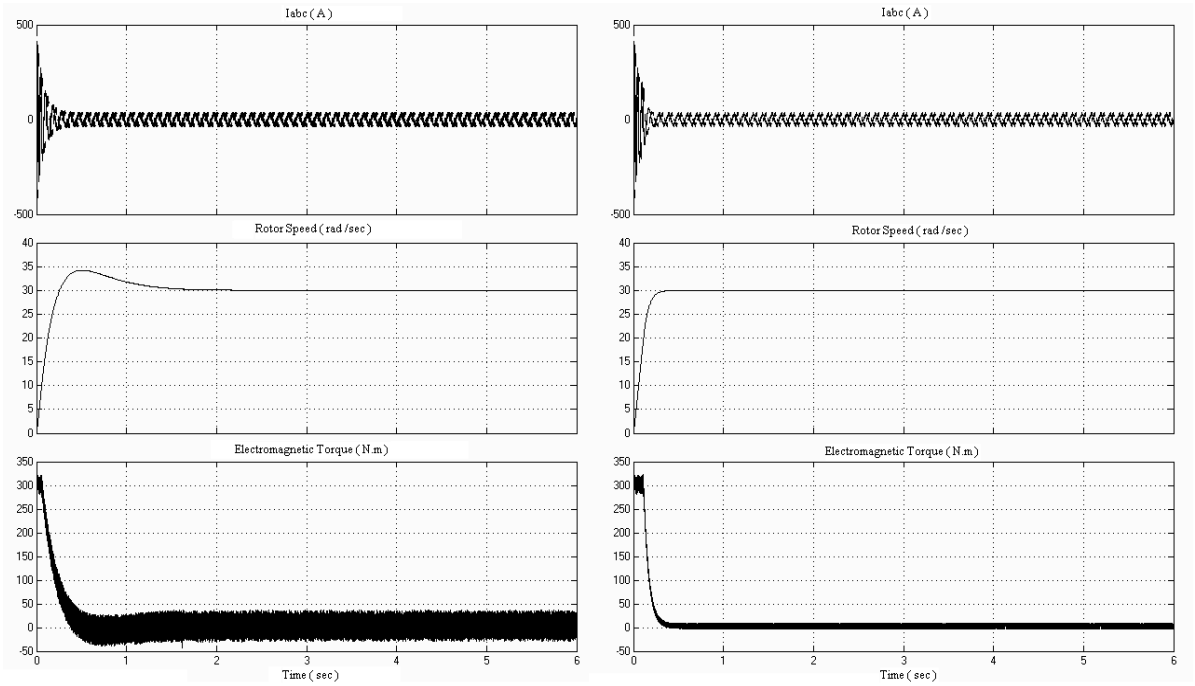

(a) PI (b) SMC-BL

Fig (14) Speed response at ω^*=30 rad/sec with no load

Fig.(15) and Fig.(16) represent the speed response for step changes of speed of the (SMC-BL) and (PI) control system for two rated speeds (120 rad/sec), (30 rad/sec) respectively. The motor speed (ω_r) tracks the reference step change model output (SMC-BL) system without overshoot and the amount of torque ripple is much less than that of the (PI) system and the speed response for the (SMC-BL) is smoother and faster than the (PI) system.

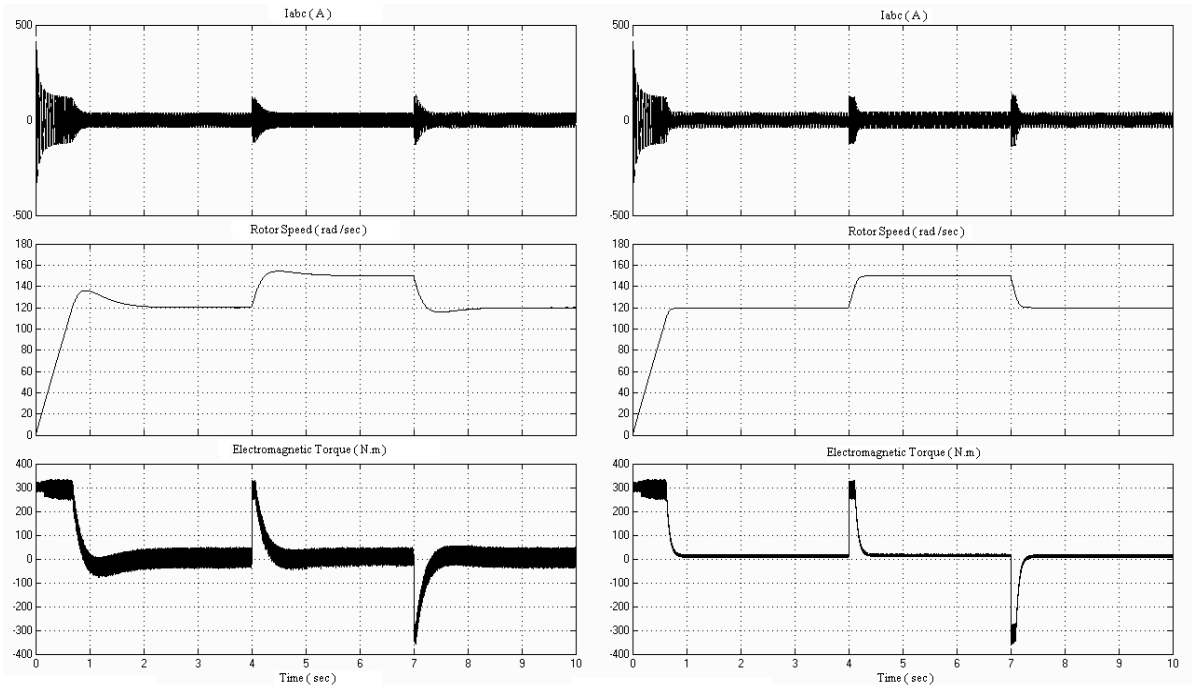

(a) PI (b) SMC-BL

Fig (15) Speed response at no load with speed step changes, at (t=4sec) from (120-150 rad/sec) and at (t=7sec) from (150-120 rad/sec).

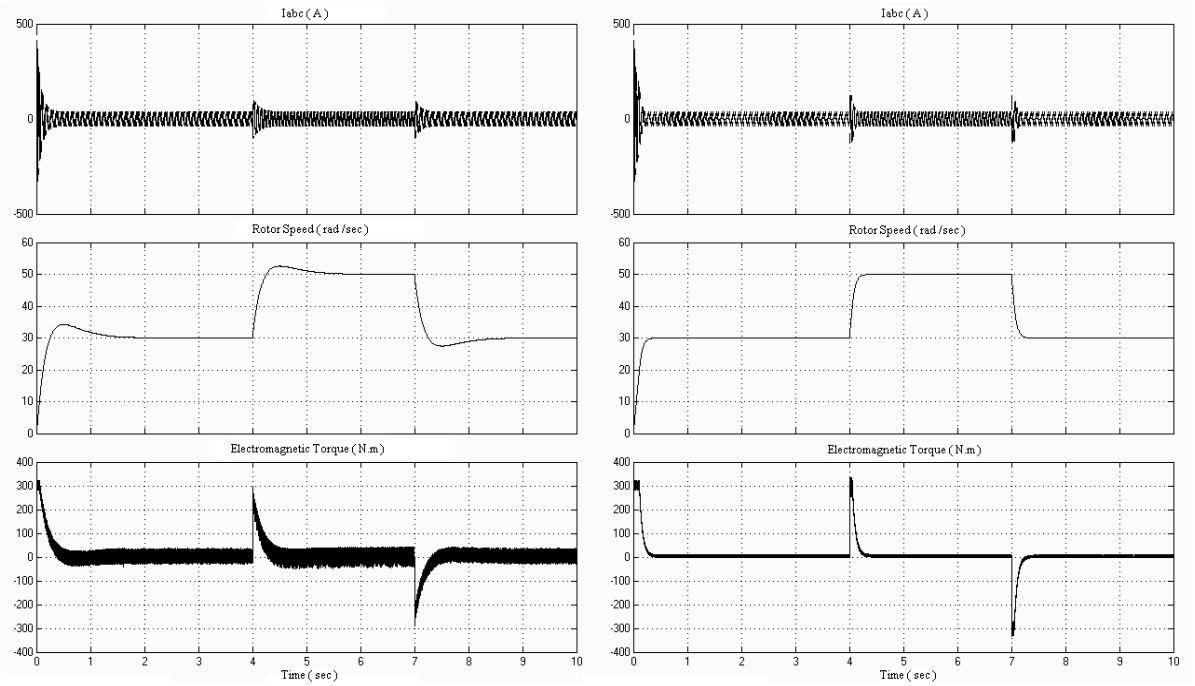

(a) PI (b) SMC-BL

Fig (16) Speed response at no load with speed step changes, at (t=4sec) from (30-50 rad/sec) and at (t=7sec) from (50-30 rad/sec).

Fig.(17) and Fig.(18) represent the speed response for forward and reverse rotating of speed of the (SMC-BL) and (PI) control system for two rated speeds (120 rad/sec), (30 rad/sec) respectively. The motor speed (ω_r) tracks the reference step change for both forward and reverse rotating case for the (SMC-BL) system without overshoot and the amount of torque ripple is much less than that of the (PI) system and the speed response for the (SMC-BL) is smoother and faster than the (PI) system.

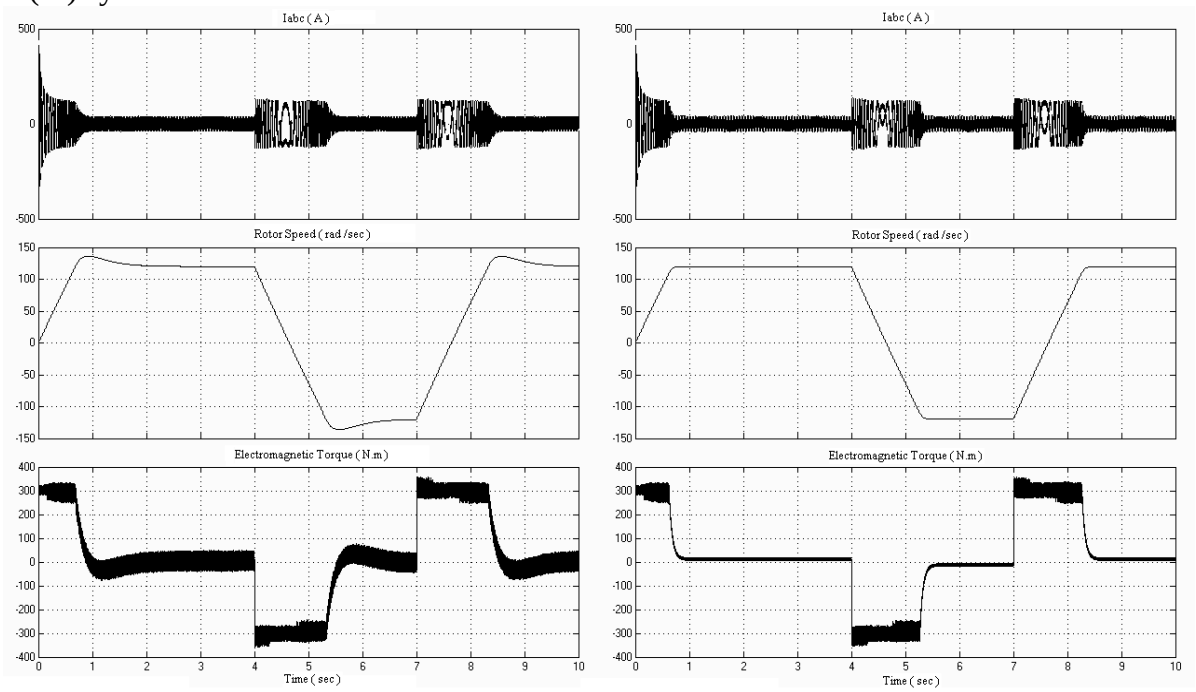

(a) PI (b) SMC-BL

Fig (17) Speed response at no load with forward and reverse speed changes, at (t=4sec) from (120 to -120 rad/sec) and at (t=7sec) from (-120 to 120 rad/sec).

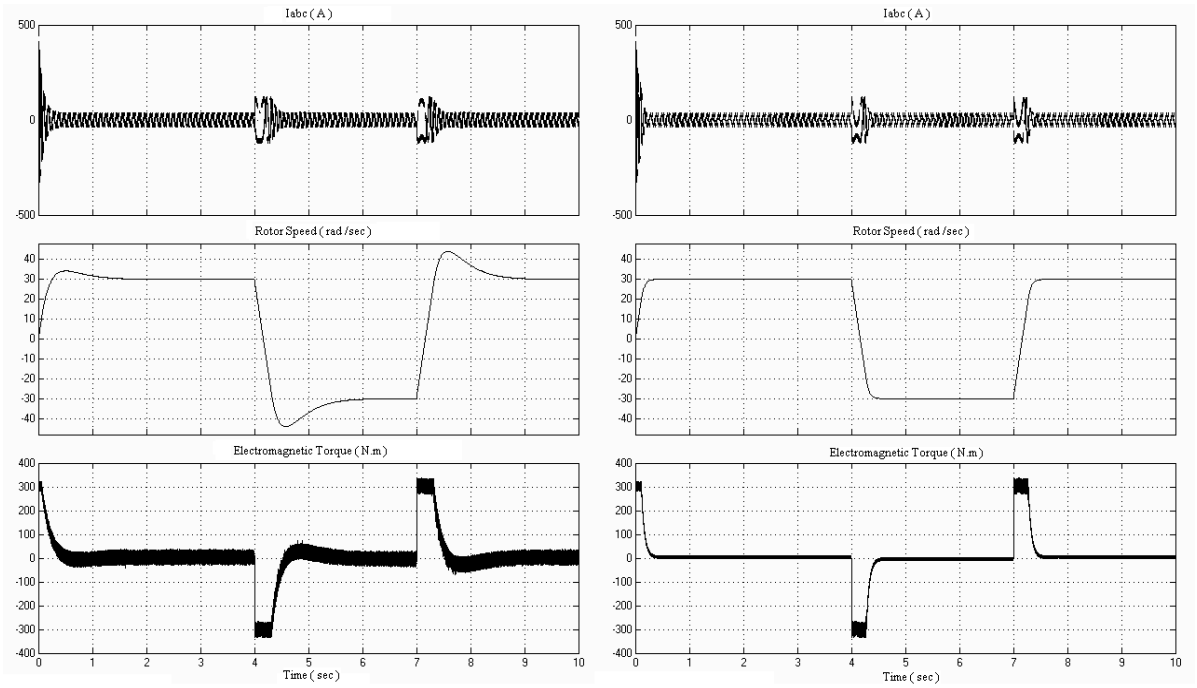

(a) PI (b) SMC-BL

Fig (18) Speed response at no load with forward and reverse speed changes, at (t=4sec) from (30 to -30 rad/sec) and at (t=7sec) from (-30 to 30 rad/sec).

System Performance under Load Conditions

Fig.(19) and Fig.(20) show the speed response for both (SMC-BL) system and (PI) system for two rated speeds (120 rad/sec), (30 rad/sec) respectively, when a set value of 200 N.m load is applied at starting. The motor speed (ω_r) tracks the reference model output (SMC-BL) system faster and without overshoot, and the amount of torque ripple at the steady state is much less than that of the (PI) system.

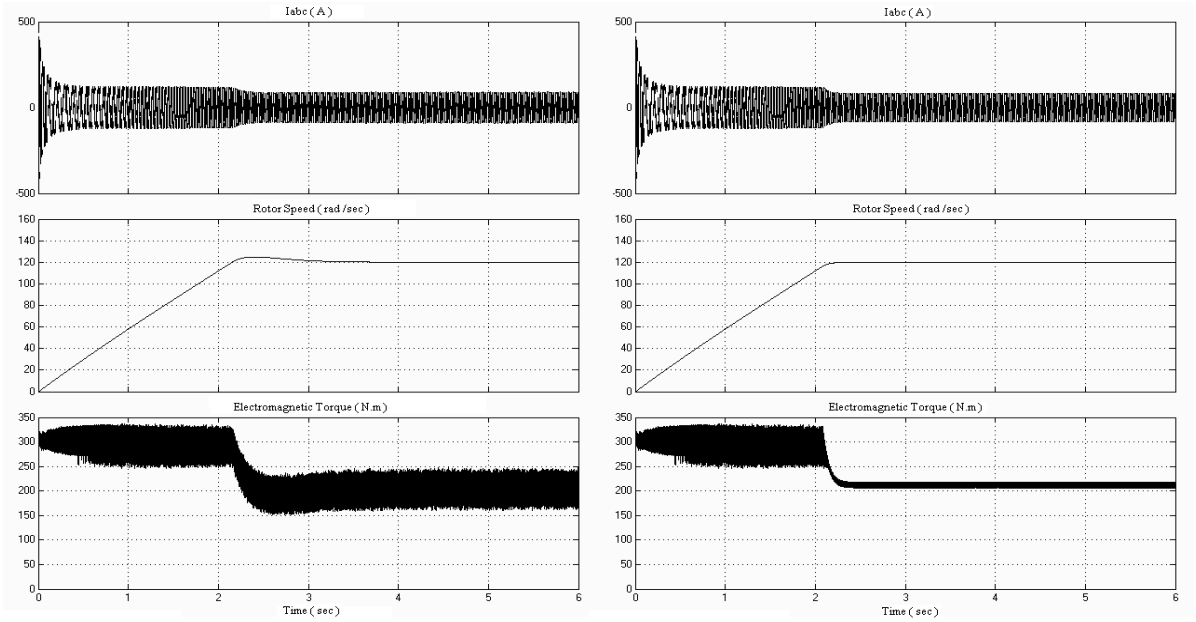

(a) PI (b) SMC-BL

Fig (19) Speed response at ω^*=120 rad/sec and constant load of 200N.m

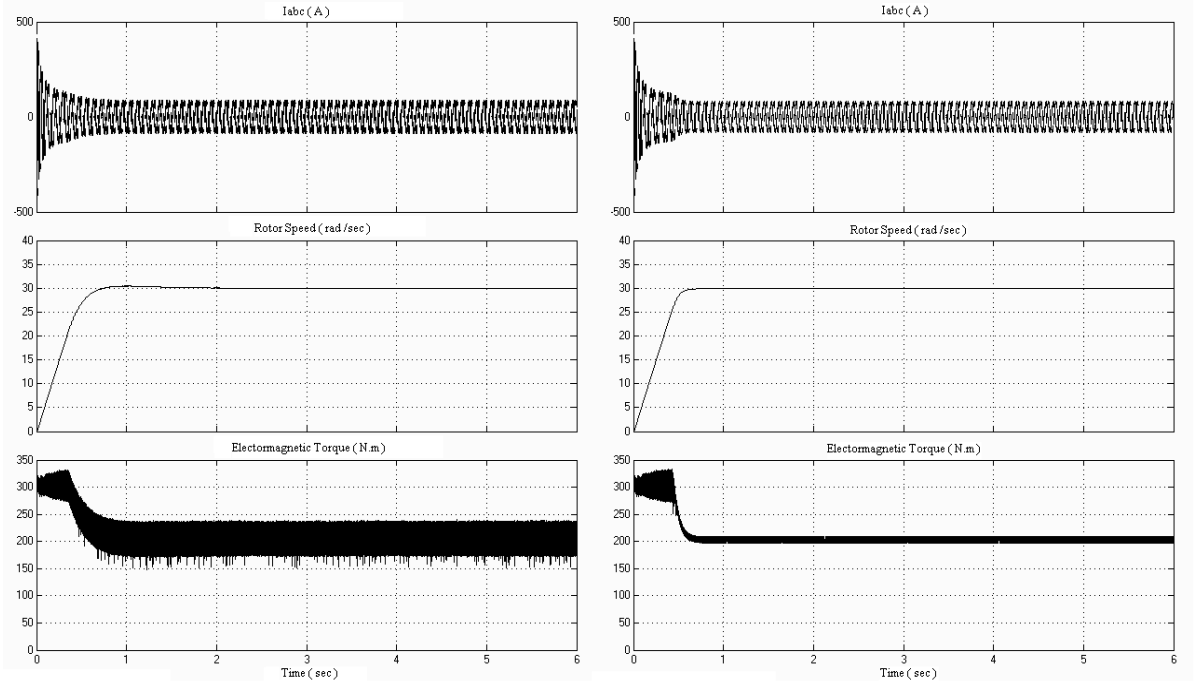

(a) PI (b) SMC-BL

Fig (20) Speed response at ω^*=30 rad/sec and constant load of 200N.m

Fig.(21) and (22) represent the speed response for step changes of load of the (SMC-BL) and (PI) control system for two speeds (120 rad/sec), (30 rad/sec) respectively. No dip or jump appears in the speed responses at the instant of applying or removing the load for the (SMC-BL) system and also the amount of torque ripple is much less than that of the (PI) system for the two rated speeds, and its obvious that the stator currents (I_{abc}) are increased when the load is applied, and the speed response for the (SMC-BL) is smoother and faster than the (PI) system.

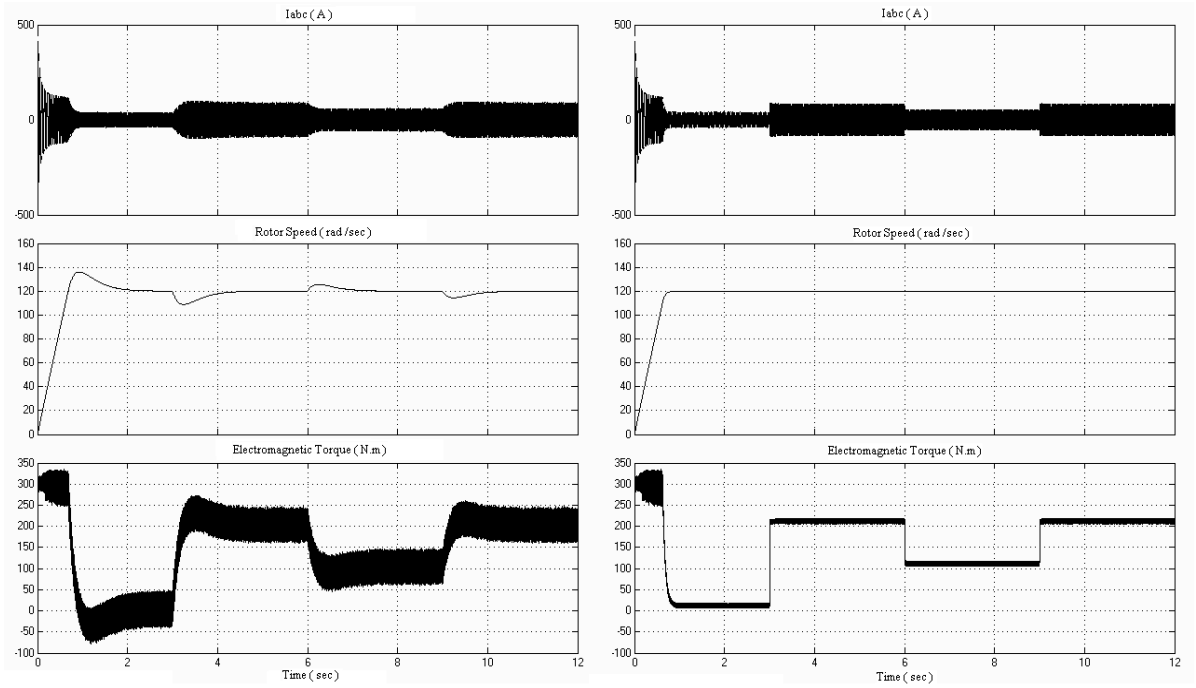

(a) PI (b) SMC-BL

Fig (21) Speed response at ω^*=120 rad/sec with load step changes, at (t=3sec) from (0-200 N.m) and at (t=6sec) from (200-100 N.m) and at (t=9sec) from (100-200 N.m).

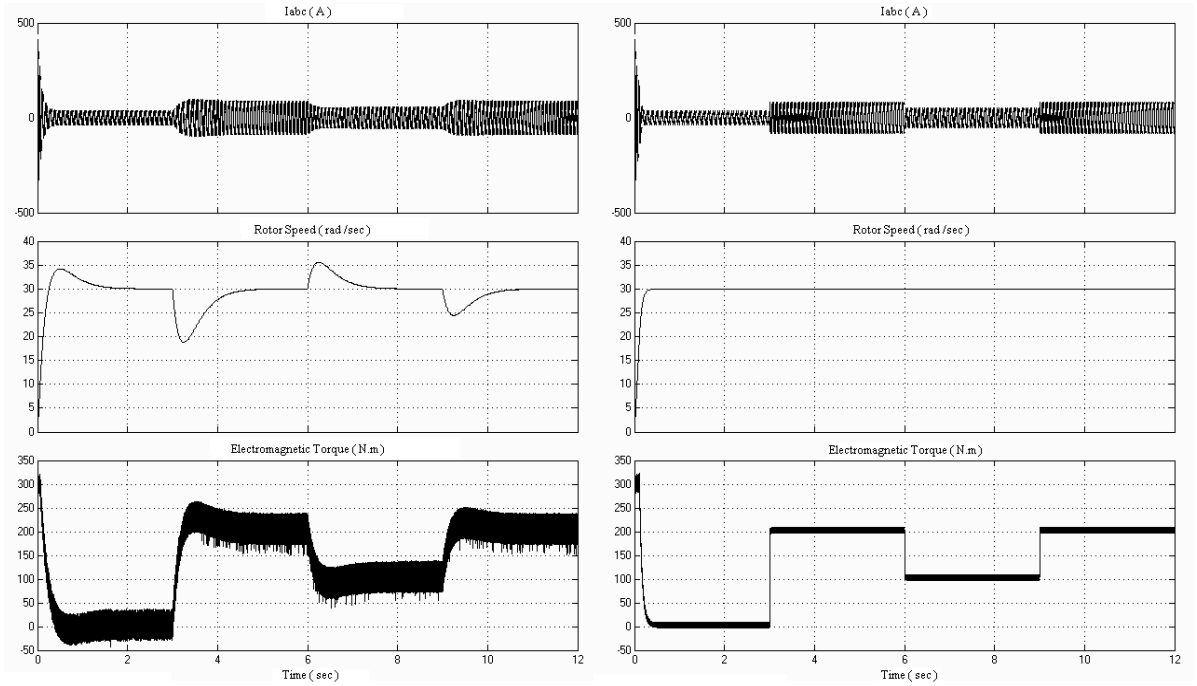

(a) PI (b) SMC-BL

Fig (22) Speed response at ω^*=30 rad/sec with load step changes, at (t=3sec) from (0-200 N.m) and at (t=6sec) from (200-100 N.m) and at (t=9sec) from (100-200 N.m).

CONCLOSIONS

Based on simulation results, the following aspects are concluded:

* The speed of the induction motor using the (SMC-BL) speed controller track the reference model output with zero steady state error and faster with no overshoot for different speeds, while the (PI) controller needs to be tuned for different speeds to insure the stability and good speed response.
* The (SMC-BL) system is more robust than the conventional system when the load disturbance occurs.
* The control techniques studied are very suitable for real time implementation due to their simplicity, robustness and ease of tuning.

REFERENCES

* B, K. Bose, ***"Modern Power Electronics and AC Drives"***, Prentice Hall Inc., USA, 2002.
* C. M. Ong, ***"Dynamic Simulation of Electric Machinery Using Matlab/Simulink"***, Prentice Hall Press, UK, 1998.
* A. M. Trzynadlowski, ***"Control of Induction Motors"***, Academic Press, UK, 2001.
* S. Emelyanov, **"*Variable Structure Control Systems*"**, Nauka Press, Moscow, Russia, 1967.
* V.I. Utkin**, "*Sliding Modes and Their Application in Variable Structure Systems*"**, Nauka Press, Moscow, Russia, 1974.
* R. A. DeCarlo, S.H Zak, and G.P. Matthews, **"*Variable Structure Control of Nonlinear Multivariable Systems: A Tutorial*",** Proceeding of IEEE, Vol.76, No.3, pp.212-232, Mar.1988.
* J. Y. Hung, W. Gao, and J. C. Hung, **"*Variable Structure Control: A Survey*",** IEEE Transactions on Industrial Electronics, Vol. 40, No.1, pp.2-22, Feb. 1993.
* Y. Itkis, **"*Control Systems of Variable Structure*"**, Wiley Press, New York, USA, 1976.

* T. V. M. Nguyen, Q. P. Ha and H. T. Nguyen, ***"A Chattering-Free Variable Structure Controller for Tracking of Robotic Manipulators"*,** Faculty of Engineering, University of Technology, Sydney, Australia, 2003.
* J. Li, **"*Design of Fuzzy Sliding-Mode Controllers and Their Applications to A Class of Mechatronic Systems* ",** Ph.D. Thesis, Department of Electrical Engineering, National Cheng Kung University Tainan, Taiwan, Repulic of China, July 2003.
* H. G. Kwatny and T. L. Siu, **"*Chattering in Variable Structure Feedback Systems*",** in Proc. IFAC 10th World Congress, Vol. 8, pp. 307-314, 1987.
* L. Zhihong, S. K. Panda, D. Q. Zhang and Y. C. Liang., ***"Modified Sliding Mode Speed Controller for Vector Controlled Induction Motor Drive"***, Proceedings of International Conference on Power Electronic Drives and Energy Systems for Industrial Growth, France, 1998.
* F. Cupertino, A. Lattanzi and L. Savatore., ***"Sliding Mode Control of an Induction Motor"***, IEE Conference on Power Electronics and Variable Speed Drives, UK, September 2000.
* A. Derdiyok, M. K. Gűven, N. Inanc, H. ur-Rehman and L. Xu., ***"A DSP – Based Indirect Field Oriented Induction Machine Control by Using Chattering–Free Sliding Mode"***, Proceedings of the IEEE National Aerospace and Electronics Conference NAECON 2000, USA, 2000.
* Y. Wang and R. Pei., ***"Speed Regulation of Induction Motor Using Sliding Mode Control Scheme"***, Conference Record of the Fourtieth Industry Applications Conference IAS Annual Meeting, USA, 2005.
* . Hazzab, I. K. Bousserhance, M. kamli and M. Rahli., ***"A New Fuzzy Sliding Mode Controller for Induction Motor Speed Control",*** IEEE Transaction on Fuzzy Systems, Vol. 7, No. 21, 2004.
* C. Gao and Y. Liu, **"*Stability of Variable Structure Control System*",** Proceeding of. American Control Conference, pp.1538-1539, Washington, USA, June 1995.
* J. E. Slotine and W. Li, **"*Applied Nonlinear Control*"**, Englewood Cliffs, Prentice Hall, Englewood cliff, new Jersey, USA, 1991.

List of symbols:

e	: Tracking error.
$\dot{e}$	: Time derivatives of the state tracking errors.
F	: Friction constant (N.m.s)
i_{qs} , i_{ds}	: q and d axis stator current (A).
i_{qr} , i_{dr}	: q and d axis rotor current (A).
I_a	: Armature current (A).
I_f	: Field current (A).
J	: Moment of inertia (Kg.m^2)
L_m	: Magnetizing inductance (H).
L_r	: Rotor inductance (H).
L_s	: Stator inductance (H).
P	: Number of machine poles
R_r	: Rotor resistance (Ω)
R_s	: Stator resistance (Ω)
$S(t)$	: Time-varying sliding surface.
$\dot{S}$	: First time-derivative of the sliding surface.
$\lvert S_i(q,t)\rvert$	: Distance between state e_i and sliding surface S_i .
T_e	: Electromagnetic Torque (N.m)

T_L	: Load torque (N.m)
v_{dr} , v_{qr}	: d and q axis rotor voltage (V).
v_{ds} , v_{qs}	: d and q axis stator voltage (V).
V	: Lyapunov function.
λ_s	: Stator flux (Wb.Turn).
λ_r	: Rotor flux (Wb.Turn).
λ_m	: Air gap flux (Wb.Turn).
λ_{qr}, λ_{dr}	: q and d axis rotor flux linkage (Wb.Turn).
λ_{qs}, λ_{ds}	: q and d axis stator flux linkage (Wb.Turn).
θ_e	: Angle between stator and rotor axes (rad).
θ_r	: Rotor position (rad)
θ_{sl}	: Slip angle (rad).
ω_r	: Angular rotor speed (electrical rad/sec).
ω_{ref}	: Desired speed (electrical rad/sec).
ω_b	: Angular Base frequency (electrical rad/sec).
ω_e	: Angular synchronous speed (electrical rad/sec).
ω_{sl}	: Slip frequency (electrical rad/sec).
Φ_i	: Boundary layer thickness.
ε_i	: Boundary layer width.